

studies were limited to a comparison of the end points of the gating conformations. The fluorescence technique described here provides information about the transition through conformational intermediates between these end points by tracking, with submillisecond resolution, the motion of specific domains of the channel protein as gating proceeds. This technique, in conjunction with labeling at other locations, should aid in the structural characterization of gating domains and shed light on conformational rearrangements that have so far been "invisible" because they neither move charge nor directly open or close the channel.

REFERENCES AND NOTES

- M. Noda *et al.*, *Nature* **312**, 121 (1984); W. A. Caterall, *Annu. Rev. Biochem.* **55**, 953 (1986); R. E. Greenblatt, T. Blatt, M. Montal, *FEBS Lett.* **193**, 125 (1985); H. R. Guy and P. Seetharamulu, *Proc. Natl. Acad. Sci. U.S.A.* **83**, 508 (1986).
- W. Stühmer *et al.*, *Nature* **339**, 597 (1989); D. M. Papazian, L. C. Timpe, Y. N. Jan, L. Y. Jan, *ibid.* **349**, 305 (1991); E. R. Liman, P. Hesse, F. W. Weaver, G. Koren, *ibid.* **353**, 752 (1991); D. E. Logothetis *et al.*, *Neuron* **8**, 531 (1992).
- N. E. Schoppa, K. McCormack, M. A. Tanouye, F. J. Sigworth, *Science* **255**, 1712 (1992).
- F. J. Sigworth, *Q. Rev. Biophys.* **27**, 1 (1994).
- N. Yang and R. Horn, *Neuron* **15**, 213 (1995).
- J. R. Lakowicz, *Principles of Fluorescence Spectroscopy* (Plenum, New York, 1983).
- S. R. Durell and H. R. Guy, *Biophys. J.* **62**, 238 (1992).
- Defolliculated, injected *Xenopus* oocytes were incubated for 3 to 4 days at 12°C, treated with 1 mM tetraglycine maleimide (TGM) in MBSH [88 mM NaCl, 1 mM KCl, 0.41 mM CaCl₂, 0.33 mM Ca(NO₃)₂, 0.82 mM MgSO₄, 2.4 mM NaHCO₃, and 10 mM Hepes (pH 7.5)] for 1 hour at 21°C to block native membrane sulphydryls, incubated for 12 to 14 hours at 21°C to permit channels to reach the plasma membrane, and labeled with 5 μM TMRM (Molecular Probes) in K⁺-MBSH [100 mM KCl, 1.5 mM MgCl₂, 0.5 mM CaCl₂, and 10 mM Hepes (pH 7.5)] for 30 min on ice. Two-electrode voltage clamping was with a Dagan CA-1 amplifier in MBSH or in NMGMES [110 mM NMGMES (N-methyl-D-glucamine methanesulfonic acid), 1 mM Ca(MES)₂, and 10 mM Hepes (pH 7.1)]. Whole-cell gating charge was calculated by subtraction of the linear capacitive component from the integral of the off-gating current. Confocal images were acquired with a Bio-Rad MRC-1000 inverted confocal microscope in photon counting mode with a 20× objective.
- E. Perozo, R. MacKinnon, F. Bezanilla, E. Stefani, *Neuron* **11**, 353 (1993).
- T. Hoshi, W. N. Zagotta, R. W. Aldrich, *Science* **250**, 533 (1990).
- A. Kamb, J. Tseng-Crank, M. A. Tanouye, *Cell* **50**, 405 (1987).
- Abbreviations for the amino acid residues are as follows: A, Ala; C, Cys; D, Asp; F, Phe; H, His; I, Ile; K, Lys; L, Leu; M, Met; N, Asn; P, Pro; Q, Gln; R, Arg; S, Ser; T, Thr; V, Val; and W, Trp.
- L. Santacruz-Tolosa, Y. Huang, S. A. John, D. M. Papazian, *Biochemistry* **33**, 5607 (1994).
- L. M. Mannuzzo, M. M. Moronne, E. Y. Isacoff, data not shown.
- L366C had a half-maximal voltage of activation of -53.8 ± 1.8 mV (mean \pm SEM; $n = 5$), indicating that channels would be mainly activated during the TMRM incubation.
- L. C. Timpe, Y. N. Jan, L. Y. Jan, *Neuron* **1**, 659 (1988); E. Y. Isacoff, D. Papazian, L. Timpe, Y. N. Jan, L. Y. Jan, *Cold Spring Harbor Symp. Quant. Biol.* **55**, 9 (1990); L. E. Iverson and B. Rudy, *J. Neurosci.* **10**, 2903 (1990); T. Hoshi, W. N. Zagotta, R. W. Aldrich, *Neuron* **7**, 547 (1991).
- Fluorescence was measured with a Hamamatsu HC120-05 photomultiplier tube connected to a Nikon DIAPHOT-TMD inverted microscope with TMD-EF Epi-Fluorescence Attachment and a Chroma High Q TRITC filter, and it was digitized at 20 kHz and low-pass filtered at 1 kHz with an 8-pole Bessel filter. Each response is an average of 5 to 10 traces.
- In solution, replacement of 50 mM KCl of K⁺-MBSH with 50 mM KI decreased peak fluorescence of 5 μM TMRM by 40%.
- E. Stefani, L. Toro, E. Perozo, F. Bezanilla, *Biophys. J.* **66**, 996 (1994); F. Bezanilla, E. Perozo, E. Stefani, *ibid.*, p. 1011; D. Sigg, E. Stefani, F. Bezanilla, *Science* **264**, 578 (1994); W. N. Zagotta, T. Hoshi, R. W. Aldrich, *J. Gen. Physiol.* **103**, 321 (1994).
- K. McCormack, W. J. Joiner, S. H. Heinemann, *Neuron* **12**, 301 (1994).
- W. N. Zagotta, T. Hoshi, J. Dittman, R. W. Aldrich, *J. Gen. Physiol.* **103**, 279 (1994).
- S. K. Aggarwal and R. MacKinnon, *Biophys. J.* **68**, A138 (1995).
- S. L. Slatin, X.-Q. Qiu, K. S. Jakes, A. Finkelstein, *Nature* **371**, 158 (1994).
- N. Unwin, *ibid.* **373**, 37 (1995).
- We thank L. Y. Jan, H. Lecar, J. Ngai, E. Reuveni, O. Baker, R. Harris, H. P. Larsson, and K. Zito for valuable discussion; A. Glazer for advice about fluorescence; G. Westheimer for advice on optical filters; and Technical Instruments Corporation for loan of fluorescence microscopy equipment. ShH4 (W434F/Δ6-46) was provided by L. Toro, and the antibody for the immunoprecipitation was provided by L. Y. Jan. Supported by American Heart Association-California Affiliate grant 94-216, by a McKnight Scholar Award to E.Y.I., and by U.S. Department of Energy contract DE-AC03-76SF00098 to M.M.M.

5 September 1995; accepted 20 November 1995

Activation of Ventrolateral Preoptic Neurons During Sleep

J. E. Sherin, P. J. Shiromani, R. W. McCarley, C. B. Saper*

The rostral hypothalamus and adjacent basal forebrain participate in the generation of sleep, but the neuronal circuitry involved in this process remains poorly characterized. Immunocytochemistry was used to identify the FOS protein, an immediate-early gene product, in a group of ventrolateral preoptic neurons that is specifically activated during sleep. The retrograde tracer cholera toxin B, in combination with FOS immunocytochemistry, was used to show that sleep-activated ventrolateral preoptic neurons innervate the tuberomammillary nucleus, a posterior hypothalamic cell group thought to participate in the modulation of arousal. This monosynaptic pathway in the hypothalamus may play a key role in determining sleep-wake states.

Clinical observations made at the beginning of this century indicated that an intact rostral hypothalamus is critical for the production of normal sleep in humans (1). Subsequent experimental studies in animals demonstrated that lesions in the preoptic area and adjacent basal forebrain (POA-BF) cause insomnia (2), whereas chemical or electrical stimulation of this region causes sleep (3, 4). Although neurons that are selectively active during sleep have been identified in the POA-BF (5, 6), no such population with an implied role in sleep generation has been anatomically characterized. Because FOS protein accumulates in recently activated neurons (7), we im-

munochemically examined the expression of FOS in the brains of 20 rats whose spontaneous sleep-wake behaviors were recorded (8), in order to identify sleep-activated cell groups. Animals were killed during the light cycle at 10:00 ($n = 8$) or 16:00 ($n = 7$) or during the dark cycle at 22:00 ($n = 5$), after which their brains were processed for immunocytochemical visualization of FOS protein (9).

In agreement with published reports (10), we observed fewer FOS-immunoreactive (FOS-ir) neurons in brains from animals that were killed during the light cycle, when rats sleep, than in brains from animals that were killed during the dark cycle, when rats are awake. However, two structures thought to mediate circadian rhythms [the intergeniculate leaflet (IGL) and the dorsal suprachiasmatic nucleus (SCNd)] and a group of cells in the ventrolateral preoptic area (VLPO) showed a pronounced and focal increase in the number of FOS-ir cells in brains from animals killed during the light cycle as compared with the dark cycle (11). Although the IGL and SCNd consistently contained numerous FOS-ir cells in the brains of all animals killed during the light cycle, the number of FOS-ir cells in the VLPO of these animals was less consistent and seemed more closely related to

J. E. Sherin, Department of Neurology, Harvard Medical School, Beth Israel Hospital, Boston, MA 02215; Program in Neuroscience, Harvard Medical School, Boston, MA 02115; and Committee on Neurobiology, University of Chicago, Chicago, IL 60637, USA.

P. J. Shiromani and R. W. McCarley, Program in Neuroscience, Harvard Medical School, Boston, MA 02115, and Department of Psychiatry, Harvard Medical School, Brockton Veterans Administration Hospital, Brockton, MA 02401, USA.

C. B. Saper, Department of Neurology, Harvard Medical School, Beth Israel Hospital, Boston, MA 02215, and Program in Neuroscience, Harvard Medical School, Boston, MA 02115, USA.

*To whom correspondence should be addressed at the Department of Neurology, Beth Israel Hospital, 330 Brookline Avenue, Boston, MA 02215, USA. E-mail: csaper@bih.harvard.edu

recent sleep experience than to circadian time. To examine the relation between FOS-ir cells in the VLPO and sleeping behavior, we counted FOS-ir cells systematically in the ventral-most sector of the lateral preoptic area of each brain and correlated the number of FOS-ir cells with the behavioral states the animals had experienced in the hour before they were killed (12, 13). Animals were coded so that cell counting and behavioral state scoring were conducted blinded to data origin.

Those rats killed during the dark cycle at 22:00 ($n = 5$), which slept an average of only $16 \pm 12\%$ (mean \pm SD) of the hour before they were killed, contained an average of 3.7 ± 1.4 (mean \pm SD) diffusely distributed FOS-ir cells per VLPO sector (Fig. 1A). Likewise, two rats that slept only 21 and 23% of the hour before they were killed in the light cycle contained just 0.5 and 7.2 FOS-ir cells per VLPO sector. The remaining rats, all killed during the light cycle ($n = 13$), slept an average of $68 \pm 19\%$ of the hour before they were killed and contained an average of 27.5 ± 11.7 FOS-ir cells per VLPO sector. FOS-ir VLPO cells were often spatially clustered (Fig. 1B) and in general were more abundant in animals that had experienced long sleeping bouts before they were killed. Plotted as a function of sleep experienced during the hour before the animal was killed, the average number of FOS-ir cells per VLPO sector increased with increasing percent total sleep time (Fig. 1D) (14). The number of FOS-ir cells in the VLPO was also examined in relation to both synchronized and desynchronized sleep as separate independent variables. However, desynchronized sleep occurred in brief, repeated bouts within

synchronized sleep epochs, thus preventing any additional correlation.

In spontaneously behaving animals the number of FOS-ir cells in the VLPO seemed to reflect a sleep-related process rather than a circadian one. But because sleeping behavior was tightly coupled to circadian time in all but two of these animals, a second experiment was carried out in which the normal relation between sleeping behavior and circadian rhythm was deliberately dissociated by depriving 33 animals of sleep for 9 hours (07:00 to 16:00; $n = 24$) or 12 hours (07:00 to 19:00; $n = 9$) of the light cycle (15). After sleep deprivation, some animals were killed immediately ($n = 5$), whereas others were killed after a recovery period ($n = 28$) during which they were permitted to sleep or wake spontaneously for 45, 90, or 180 min before they were killed. Brain tissue was then processed for immunocytochemical visualization of FOS protein. Sleep scoring and analysis of FOS-ir staining were as described previously (12).

The sleep-deprivation experiments succeeded in dissociating sleeping and the expression of FOS in the VLPO from the circadian rhythm. In the SCN and IGL, for example, the pattern of FOS-ir staining followed the light-dark cycle, as in spontaneously behaving animals. In contrast, FOS staining in the VLPO reflected recent sleep experience with no significant differences between the 9-hour and 12-hour sleep deprivation groups. Thus, animals that were killed immediately after 9 hours of sleep deprivation (in the light cycle; $n = 3$) and animals killed immediately after 12 hours of sleep deprivation (in the dark cycle; $n = 2$) contained 6.3 ± 3.2 FOS-ir cells per VLPO

sector. In contrast, animals allowed to recover from 9 hours ($n = 21$) and 12 hours ($n = 7$) of sleep deprivation slept $64 \pm 23\%$ of the hour before they were killed and contained 25.6 ± 9.9 FOS-ir cells per VLPO sector. As in spontaneously sleeping animals, the FOS-ir cells in the VLPO of animals allowed to recover after sleep deprivation were often spatially clustered (Fig. 1C) and in general were more abundant in animals that experienced long sleeping bouts before they were killed. Plotted as a function of sleep experienced during the hour before the animal was killed, the average number of FOS-ir cells per VLPO sector increased with increasing percentage

Fig. 1. (A to C) Photomicrographs of FOS-immunostained coronal sections through the preoptic hypothalamus of spontaneously behaving rats that slept 15% (A) and 63% (B), and a sleep-deprived rat that slept 83% (C) of the hour before they were killed; FOS-ir cells (black nuclei) are apparent in the VLPO of animals that slept most of the hour before they were killed (B and C; arrows). **(D)** Correlation between the number of FOS-ir cells counted in each preoptic sector containing the VLPO [shown in (A)] and percent of total sleep time for spontaneously behaving rats (closed circles; solid regression line; $R = 0.743$, $P < 0.0001$) and sleep-deprived rats (open circles; dashed regression line; $R = 0.704$, $P < 0.0001$). OC, optic chiasm. Scale bar, 150 μ m.

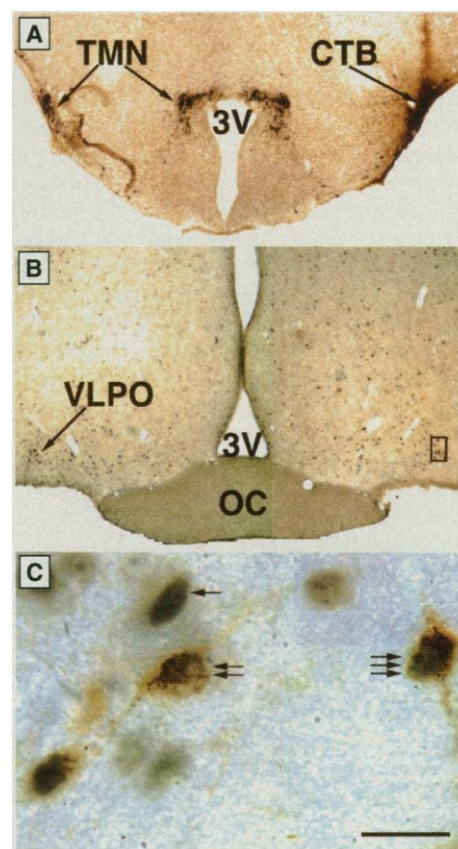
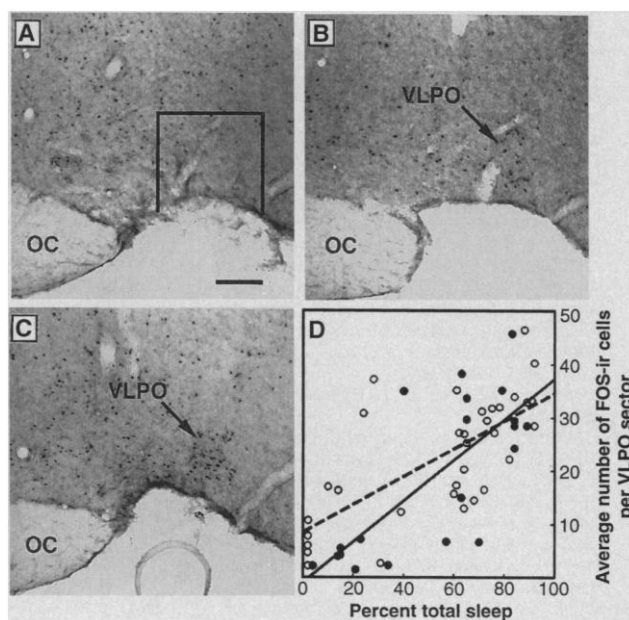


Fig. 2. (A) Photomontage of a coronal section through the posterior hypothalamus showing dorsomedial and ventrolateral components of the TMN (black) as delineated with an antibody against adenosine deaminase. CTB (brown) is shown deposited into the right ventrolateral TMN, where a large cluster of histaminergic neurons is located. **(B)** Photomontage of a coronal section through the preoptic hypothalamus of an animal that received a CTB injection into the TMN region [depicted in (A)] and then was killed 1 week later at 10:00. **(C)** High-power photomontage of immunostained neurons from the boxed field in (B) rotated clockwise 90°, demonstrating a singly labeled FOS-ir cell (black nucleus; single arrow), a singly labeled CTB-ir cell (brown cytoplasm; two arrows), and a doubly labeled cell (black nucleus and brown cytoplasm; three arrows) in the VLPO. OC, optic chiasm; 3V, third ventricle. Scale bar, 1.6 mm in (A), 400 μ m in (B), and 40 μ m in (C).

of total sleep time (14). The paucity of FOS-ir cells in the VLPO of sleep-deprived animals killed without sleep recovery also illustrates that FOS immunoreactivity in cells of the VLPO is not related to the need for sleep [which is highest after forced waking (16)] but to sleeping.

With the exception of the SCN and IGL, where FOS staining reflects circadian time, our observations indicate that the number of FOS-ir neurons throughout the brain declines during sleep (10) at the same time that it increases in a discrete collection of VLPO cells. Because FOS immunoreactivity has been shown to reflect recent neuronal activation (7), we propose that VLPO cells that accumulate FOS protein during sleep may constitute a subpopulation of the sleep-active neurons in the POA-BF that have been postulated to participate in the generation of sleeping behavior (5, 6).

One potential mechanism of sleep generation by the POA-BF is suggested by the observation that many inhibitory neurons in this region innervate posterolateral hypothalamic cells that (by way of extensive projections to cortex) are thought to participate in arousal (17). In particular, we have shown that neurons in the VLPO specifically innervate cell bodies and proximal dendrites of histaminergic cells in the ipsilateral tuberomammillary nucleus (TMN) (18). Because histaminergic neurons in the TMN are considered to be a critical component of the posterolateral hypothalamic arousal system (19), we investigated whether the TMN is innervated by sleep-activated VLPO cells. We injected the retrograde tracer cholera toxin subunit B (CTB) into the TMN region of 15 rats (20). Five to 7 days later animals were killed as before at 10:00 after spontaneous sleep bouts. Preoptic tissue was then processed immunocytochemically for CTB and FOS protein while injection sites were determined by processing posterior hypothalamic tissue immunocytochemically for CTB and adenosine deaminase, an enzyme that is coexpressed with histamine in TMN neurons (21). CTB injections into sites that did not include the TMN did not produce retrograde labeling in the VLPO. However, each of three animals injected with CTB into sites that included the TMN contained retrogradely labeled neurons in the ipsilateral VLPO, roughly half of which contained FOS-ir nuclei. One such case, in which the ventrolateral component of the TMN on one side was filled with CTB (Fig. 2A), produced 20 retrogradely labeled ipsilateral VLPO cells (from a one in four series; 40 μ m), 15 of which were FOS-ir. Thus, VLPO neurons that accumulate FOS protein during sleep provide direct input to the histaminergic complex (Fig. 2, B and C).

Histaminergic neurons (like other aminergic cell groups thought to promote arousal)

are tonically active during waking, become less active during slow wave sleep, and cease firing during rapid eye movement (REM) sleep (22). Because the activity of histaminergic neurons is thought to modulate arousal, the VLPO cells described here are strategically positioned to modulate sleep-wake behaviors through state-specific synaptic inputs to histaminergic neurons. Although the neurotransmitter used in this pathway is not known, recent microdialysis data demonstrate that during sleep, λ -aminobutyric acid (GABA) levels in the posterior hypothalamus are increased (23). Injection of a GABA agonist into the TMN region has been shown to restore sleep in preoptic lesioned, otherwise insomniac, cats (24). In addition, electrical stimulation of POA-BF sites in the horizontal hypothalamic slice preparation produces GABA_A-mediated fast inhibitory postsynaptic potentials in histaminergic neurons (25). Lastly, ultrastructural studies have shown that histaminergic cell bodies and proximal dendrites are contacted by GABA-ergic terminals of unknown origin (26). These observations suggest that the histaminergic system (which promotes arousal during wakefulness) is inhibited during sleep by GABA-ergic inputs that originate in the VLPO (2, 27). Such a relation between the anterior and posterior hypothalamus, predicted by the work of Nauta almost 50 years ago [in (2)], may be key to the mechanism by which the hypothalamus influences sleep-wake state.

REFERENCES AND NOTES

1. L. Mauthner, *Wien. Med. Wochenschr.* **40**, 961 (1890); C. von Economo, *J. Nerv. Ment. Dis.* **71**, 249 (1930); reviewed by M. B. Sterman and M. N. Shouse, in *Brain Mechanisms of Sleep*, D. J. McGinty, Ed. (Raven, New York, 1985), pp. 277-299.
2. W. J. H. Nauta, *J. Neurophysiol.* **9**, 285 (1946); D. McGinty and M. B. Sterman, *Science* **160**, 1253 (1968); E. A. Lucas and M. B. Sterman, *Exp. Neurol.* **46**, 368 (1975); R. Szymusiak and D. McGinty, *ibid.* **94**, 598 (1986); M. Sallan et al., *Neuroscience* **32**, 669 (1989).
3. B. R. Kaada, *Acta. Physiol. Scand.* **24** (suppl. 83), 200 (1951); M. B. Sterman and C. D. Clemente, *Exp. Neurol.* **6**, 91 (1962); W. W. Roberts and T. C. L. Robinson, *ibid.* **25**, 282 (1969); R. Ueno, Y. Ishikawa, T. Nakayama, O. Hayaishi, *Biochem. Biophys. Res. Commun.* **109**, 576 (1982); L. E. Garcia-Ararras and J. R. Pappenheimer, *J. Neurophysiol.* **49**, 528 (1983); W. B. Mendelson, J. V. Martin, M. Perlis, R. Wagner, *Neuropsychopharmacology* **2**, 61 (1989); Y. Koyama and O. Hayaishi, *Brain Res. Bull.* **33**, 367 (1994); H. Matsumura et al., *Proc. Natl. Acad. Sci. U.S.A.* **91**, 11998 (1994).
4. D. McGinty, R. Szymusiak, D. Thompson, *Brain Res.* **667**, 273 (1994).
5. A. L. Findlay and J. N. Hayward, *J. Physiol.* **201**, 237 (1969); B. N. Mallick, G. S. China, K. R. Sundaram, B. Singh, V. Mohan Kumar, *Exp. Neurol.* **81**, 586 (1983); K. I. Kaitin, *ibid.* **83**, 347 (1984); L. Detari, G. Juhasz, T. Kukorelli, *Electroencephalogr. Clin. Neurophysiol.* **59**, 362 (1984); R. Szymusiak and D. McGinty, *Brain Res.* **370**, 82 (1986); Y. Ogawa and H. Kawamura, *Brain Res. Bull.* **20**, 897 (1988).
6. M. N. Alam, D. McGinty, R. Szymusiak, *Am. J. Physiol.*, in press.
7. S. M. Sagar, F. R. Sharpe, T. Curran, *Science* **240**, 1328 (1988); M. Dragunow and R. Faull, *J. Neurosci. Methods* **29**, 261 (1989); M. Sheng and M. E. Greenberg, *Neuron* **4**, 477 (1990).
8. In anesthetized rats (acepromazine, 0.75 mg per kilogram of body weight; ketamine, 44.0 mg/kg; xylazine, 2.5 mg/kg), screw electrodes were implanted in the skull to record the electroencephalogram (EEG), and flexible wires were placed in the nuchal muscles to record the electromyogram (EMG). After attachment to Amphenol connectors, the apparatus was fixed in place with dental cement. Rats were housed individually at 24°C with food and water provided ad libitum and lights on from 07:00 to 19:00 (light cycle) and off from 19:00 to 07:00 (dark cycle). One week after surgery, rats were connected by means of flexible wires to a Grass electroencephalograph (model 79) for recording EEG and EMG. Rats were adapted to the setup for 3 days during which sample sleep recordings were obtained. Experimental sessions consisted of connecting animals for recording (as during adaptation of three previous days) until they were killed.
9. Anesthetized rats (5) were perfused transcardially with 0.9% saline (50 ml) followed by 10% formalin in 0.1 M phosphate buffer (500 ml; pH 7.4). Brains were postfixed in situ for 6 hours at 4°C, were removed and placed into 20% sucrose in 0.1 M phosphate buffer until they sank, and then were cut on a freezing microtome at 40 μ m. Sections were processed for FOS immunocytochemistry as described [J. K. Elmquist et al., *Endocrinology* **133**, 3054 (1993)], with antibody to FOS as primary antibody (Oncogene Sciences Ab 2; 1:5000 dilution) and Co²⁺-enhanced diaminobenzidine (DAB) as chromagen (black nuclear reaction product). This NH₂-terminally directed polyclonal antibody has been shown to stain the FOS protein specifically [G. E. Hoffman, M. S. Smith, J. G. Verbalis, *Front. Endocrinol.* **3**, 173 (1993)].
10. J. Kononen, J. Koistinaho, H. Alho, *Neurosci. Lett.* **120**, 105 (1990); C. Cirelli, M. Pompeiano, G. Tonini, *Arch. Ital. Biol.* **131**, 327 (1993); M. Bentivoglio et al., *Sleep Res.* **22**, 475 (1993); G. Grassi-Zucconi et al., *ibid.*, p. 478; M. Pompeiano, C. Cirelli, G. Tonini, *J. Sleep Res.* **3**, 80 (1994); G. Grassi-Zucconi et al., *J. Physiol. Paris* **88**, 91 (1994).
11. Because the IGL, SCN, and VLPO contained only a few FOS-ir neurons in dark cycle (waking) animals, increased staining in light cycle (sleeping) animals in these regions was quite conspicuous. Although FOS staining generally decreased during the light cycle in the rest of the brain, some areas, including the cingulate cortex, piriform cortex, paraventricular thalamus, and medial preoptic area, contained FOS-ir cells under all conditions. We focused on the SCN, IGL, and VLPO because they were the only cell groups with a clear-cut increase in FOS staining during the light cycle. We cannot, however, eliminate the possibility that neurons scattered in other cell groups accumulate FOS during the light cycle.
12. The VLPO was demarcated for FOS quantification in a coronal plane approximating that in the Paxinos rat brain atlas. Beginning at the rostral pole of the supraoptic and suprachiasmatic nuclei and continuing rostrally, six 40- μ m sections were analyzed bilaterally from a one in two series, such that 12 VLPO sectors were counted and averaged for each brain. Each VLPO sector was demarcated by the base of the brain and extended dorsally 0.3 mm and laterally from 1.0 mm lateral to the midline to the edge of the olfactory tubercle (box in Fig. 1A). Behaviors for the hour before the rat was killed (when FOS protein approaches maximal levels in activated neurons [P. J. Shiromani et al., *Mol. Brain Res.* **29**, 163 (1995)]) were scored manually by EEG and EMG criteria as percentages of waking, synchronized, and desynchronized sleep. The percentage of time spent in synchronized and desynchronized sleep was combined to obtain percent total sleep time values.
13. Mean (\pm SD) of percent total sleep time for animals in this study was 63 \pm 22 for rats killed at 10:00, 67 \pm 24 for rats killed at 16:00, and 16 \pm 12 for rats killed at 22:00; these values are within published norms [Z. J. M. Van Hulzen and H. M. L. Coenen, *Physiol. Behav.* **25**, 807 (1980)].
14. Pearson correlation coefficients were used to deter-

- mine the significance of the relation between the number of FOS-ir cells in the VLPO and percent total sleep time [G. W. Snedecor and W. G. Cochran, *Statistical Methods* (Iowa State Univ. Press, Ames, IA, 1989), pp. 177–195.
15. EEG and EMG recordings were monitored continuously. When animals showed evidence of sleep they were aroused by gentle prodding.
 16. A. A. Boberly and I. Tobler, in *Brain Mechanisms of Sleep*, D. J. McGinty, Ed. (Raven, New York, 1985), pp. 35–44.
 17. I. Gritti, L. Mairville, B. E. Jones, *J. Comp. Neurol.* **339**, 251 (1994).
 18. J. E. Sherin, R. Burstein, C. B. Saper, *Soc. Neurosci. Abstr.* **19**, 31 (1993); J. E. Sherin and C. B. Saper, in preparation.
 19. B. J. Wilcox and V. S. Seybold, *Neurosci. Lett.* **20**, 105 (1982); T. Watanabe *et al.*, *ibid.* **39**, 249 (1983); P. Panula, H.-Y.T. Yang, E. Costa, *Proc. Natl. Acad. Sci. U.S.A.* **81**, 2572 (1984); C. P. Swett and J. A. Hobson, *Arch. Ital. Biol.* **106**, 279 (1968); J. S. Lin, K. Sakai, M. Jouvet, *Neuropharmacology* **27**, 111 (1988); J. C. Schwartz, J. M. Arrang, M. Garbarg, H. Pollard, M. Ruat, *Physiol. Rev.* **71**, 1 (1991); J. Monti, *Life Sci.* **53**, 1331 (1993).
 20. By means of an air-pressure delivery system, 1% CTB dissolved in 0.9% saline (~1 nl) was injected stereotaxically through a glass micropipette into the TMN region of chloral hydrate-anesthetized rats (350 mg/kg). Coordinates from the Paxinos rat atlas were: AP, -4.0 mm (from bregma); DV, -9.0 mm (from cortical surface); and RL, +1.5 mm (from midline).
 21. After processing preoptic tissue for FOS immunoreactivity to identify activated cells (Co²⁺-enhanced DAB; black nuclei), and posterior hypothalamic tissue for adenosine deaminase immunoreactivity (1:50,000) to delineate the tuberomammillary nucleus for injection site localization (Co²⁺-enhanced DAB; black cell bodies) [E. Senba *et al.*, *J. Neurosci.* **5**, 3393 (1985)], sections were incubated for 18 hours at room temperature in goat anti-CTB primary antibody (List Biol. Labs, 1:100,000), followed by a 2-hour incubation in biotinylated donkey anti-goat secondary antibody (Jackson, 1:1000). An ABC kit (Vector Labs, 1:500) was used to visualize retrograde CTB labeling and CTB injection sites (DAB alone; brown cytoplasmic granules).
 22. G. Vanni-Mercier, K. Sakai, M. Jouvet, *C.R. Acad. Sci. Paris* **298**, 195 (1984); R. Szymusiak, T. Iriye, D. McGinty, *Brain Res. Bull.* **23**, 111 (1989); reviewed in M. Steriade and R. McCarley, *Brainstem Control of Wakefulness and Sleep* (Plenum, New York, 1990).
 23. D. N. Nitz and J. M. Siegel, *Sleep Res.* **24**, 12 (1995).
 24. J. S. Lin, K. Sakai, G. Vanni-Mercier, M. Jouvet, *Brain Res.* **479**, 225 (1989).
 25. O. Z. Yang and G. I. Hattton, *Soc. Neurosci. Abstr.* **20**, 346 (1994).
 26. H. Ericson, C. Kohler, A. Blomqvist, *J. Comp. Neurol.* **305**, 462 (1991).
 27. R. Szymusiak and D. McGinty, *Brain Res.* **498**, 355 (1989); B. L. Kriowicz, R. Szymusiak, D. McGinty, *ibid.* **668**, 30 (1994).
 28. We thank Q.-H. Ha and M. Magner for technical assistance, R. Burstein, J. Elmquist, T. Scammel, M. Greenberg, and J. A. Hobson for helpful discussions, and R. Kellems for ADA antiserum. Supported by USPHS grants NS22835, MH10709, and NS30140 and by a Grant-in-aid from the American Heart Association (94013110) and the Department of Veterans Affairs Medical Research Service.

7 June 1995; accepted 24 October 1995

Plasmodium Hemozoin Formation Mediated by Histidine-Rich Proteins

David J. Sullivan Jr., Ilya Y. Gluzman, Daniel E. Goldberg*

The digestive vacuole of *Plasmodium falciparum* is the site of hemoglobin degradation, heme polymerization into crystalline hemozoin, and antimalarial drug accumulation. Antibodies identified histidine-rich protein II (HRP II) in purified digestive vacuoles. Recombinant or native HRP II promoted the formation of hemozoin, and chloroquine inhibited the reaction. The related HRP III also polymerized heme, and an additional HRP was identified in vacuoles. It is proposed that after secretion by the parasite into the host erythrocyte cytosol, HRPs are brought into the acidic digestive vacuole along with hemoglobin. After hemoglobin proteolysis, HRPs bind the liberated heme and mediate hemozoin formation.

Plasmodium falciparum, the etiologic agent of severe malaria, ingests more than 75% of its host cell hemoglobin in a short period during the trophozoite stage of its intraerythrocytic cycle (1). Proteolysis occurs inside an acidified digestive vacuole where aspartic and cysteine proteases degrade the hemoglobin, releasing the toxic heme moiety (2). Lacking heme oxygenase, plasmodia detoxify heme by polymerization into an insoluble crystalline substance called hemozoin (3), in which the iron of one heme is coordinated to the propionate carboxylate group of the next heme (4). Hemozoin can be made in vitro by adding whole trophozoite lysate to acidified heme at pH 5 to 6 (5). The observed properties of this reaction suggested the existence of an enzymatic activity, but the identification and purification of the proposed enzyme (named heme

polymerase) have remained elusive. Hemozoin appears to be structurally identical to β -hematin (4), which can form spontaneously under nonphysiological conditions without the addition of protein (6). Purified hemozoin devoid of proteins or β -hematin can seed the polymerization reaction under more physiological conditions (7); this finding raised the possibility that hemozoin formation may be a nonenzymatic process, but it shed no light on the mechanism of initiation of heme polymerization before the first crystals exist. Chloroquine, a mainstay of antimalarial therapy, inhibits hemozoin formation during chemical synthesis (6), hemozoin-initiated reaction (7), or trophozoite extract-mediated production (5). In vivo, the consequences of free heme accumulation during chloroquine treatment are membrane lysis (8) and inactivation of the hemoglobin-degrading proteases (9). This appears to be the mechanism of action of 4-aminoquinoline antimalarials (5, 10).

When a ring-stage complementary DNA (cDNA) *P. falciparum* library was screened with rabbit antiserum to purified digestive vacuoles or to hemozoin (11), 67 of 104

clones that were isolated encoded the sequence for HRP II. A specific monoclonal antibody (mAb) identified HRP II in purified digestive vacuoles by both protein immunoblot and immunofluorescence (Fig. 1, A and B). In contrast, neither preimmune sera nor antibody to knob-associated HRP I recognized the vacuoles. In whole intraerythrocytic trophozoites, the previously reported pattern of intense HRP II staining of the erythrocyte cytosol and paucity of staining in the trophozoite (12) was confirmed. However, staining could also be seen internal to the parasite, over the digestive vacuole (Fig. 1C). Thus, a substantial portion of the parasite's HRP II is internalized into the digestive vacuole. This new route contrasts with HRP II's previously established path of secretion into the bloodstream, which forms the basis of the recent ParaSight test that detects HRP II in lysed finger-prick samples (13).

HRP II contains 51 repeats of the tripeptide His-His-Ala (14); together, histidine and alanine make up 76% of the mature protein. Recent work with human histidine-rich glycoprotein (HRG) demonstrated the existence of a heme-binding site in the histidine-rich domain (15). Its heme-binding motif, Gly-His-His-Pro-His-Gly (16), has similarities to the repetitive HRP II sequence Ala-His-His-Ala-His-His-Ala-Ala-Asp (14). We hypothesized that HRP II could bind heme in the digestive vacuole and might play a role in hemozoin formation. To examine this hypothesis, we ligated a cDNA clone of HRP II in-frame into a pET 15b vector for *Escherichia coli* expression (17). The recombinant protein was collected by nickel chelation chromatography. Similarly, native HRP II was purified from *Plasmodium* culture supernates (18). Each molecule of HRP II bound an estimated 17 molecules of heme in 100 mM sodium acetate at pH 4.8 (Fig. 2A). In an in vitro

Howard Hughes Medical Institute, Departments of Medicine and Molecular Microbiology, Washington University School of Medicine, and Jewish Hospital of St. Louis, Post Office Box 8230, 660 South Euclid Avenue, St. Louis, MO 63110, USA.

*To whom correspondence should be addressed. E-mail: goldberg@borcim.wustl.edu